**Supplementary Information**

# Loss-of-function mutations of *SCN10A* encoding $Na_V1.8$ α subunit of voltage-gated sodium channel in patients with human kidney stone disease

Choochai Nettuwakul[1,9], Oranud Praditsap[2,3,9], Nunghathai Sawasdee[1], Nanyawan Rungroj[2], Katesirin Ruamyod[4], Wattana B Watanapa[4], Mutita Junking[1], Sittideth Sangnual[1], Suchai Sritippayawan[5], Boonyarit Cheunsuchon[6], Duangporn Chuawattana[5], Santi Rojsatapong[7], Wipada Chaowagul[7], Sulayman D Dib-Hajj[8], Stephen G Waxman[8], and Pa-thai Yenchitsomanus[1,*]

[1] Division of Molecular Medicine, Department of Research and Development, Faculty of Medicine Siriraj Hospital, Mahidol University, Bangkok 10700, Thailand;
[2] Division of Molecular Genetics, Department of Research and Development, Faculty of Medicine Siriraj Hospital, Mahidol University, Bangkok 10700, Thailand;
[3] Immunology Graduate Program and Department of Immunology, Faculty of Medicine Siriraj Hospital, Mahidol University, Bangkok 10700, Thailand;
[4] Department of Physiology, Faculty of Medicine, Siriraj Hospital, Mahidol University, Bangkok 10700, Thailand;
[5] Division of Nephrology, Department of Medicine, Faculty of Medicine Siriraj Hospital, Mahidol University, Bangkok 10700, Thailand;
[6] Department of Pathology, Faculty of Medicine Siriraj Hospital, Mahidol University, Bangkok 10700, Thailand;
[7] Department of Medicine, Sappasithiprasong Hospital, Ubon Ratchathani 34000, Thailand;
[8] Department of Neurology & The Center for Neuroscience and Regeneration Research, Yale University School of Medicine, New Haven, CT, 06516, USA

***Correspondence:** Prof. Pa-thai Yenchitsomanus, Division of Molecular Medicine, Department of Research and Development, Faculty of Medicine Siriraj Hospital, Mahidol University, Bangkok 10700, Thailand. Email: pathai.yen@mahidol.ac.th or ptyench@gmail.com

[9] These authors contributed equally to this work.

**Supplementary figures and legends**

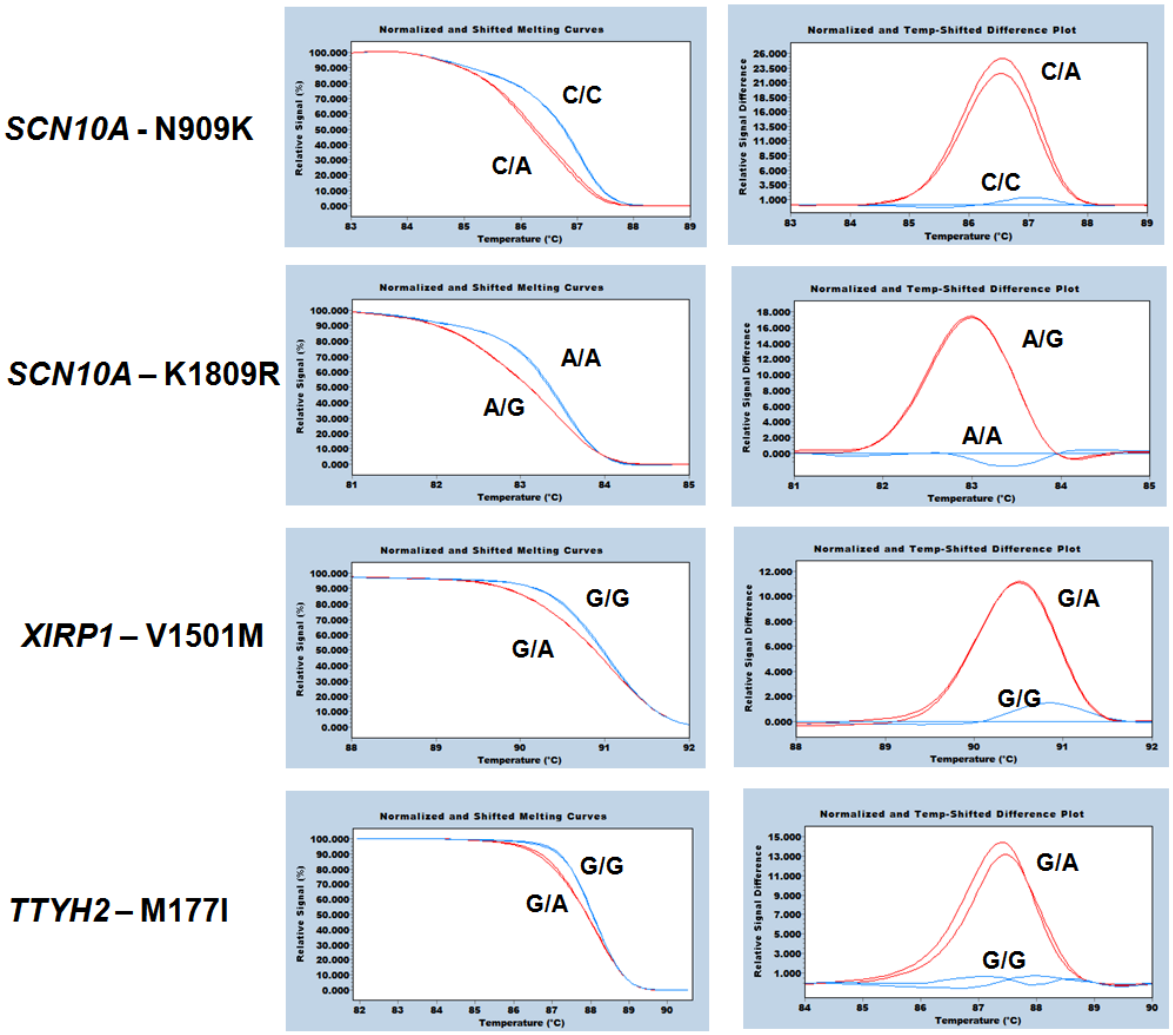


**Figure S1.** Genotyping of four variations, including two rare variations in *SCN10A* (rs567269429 and rs561166361; p.N909K and p.K1809R), one reported variation in *XIRP1* (rs58805228; p.V1501M), and one rare variation in *TTYH2* (rs371502920; p.M177I) by PCR-HRM method, showing melting curves and difference plots of amplicons from samples with either homozygous wild-types or heterozygous variants.

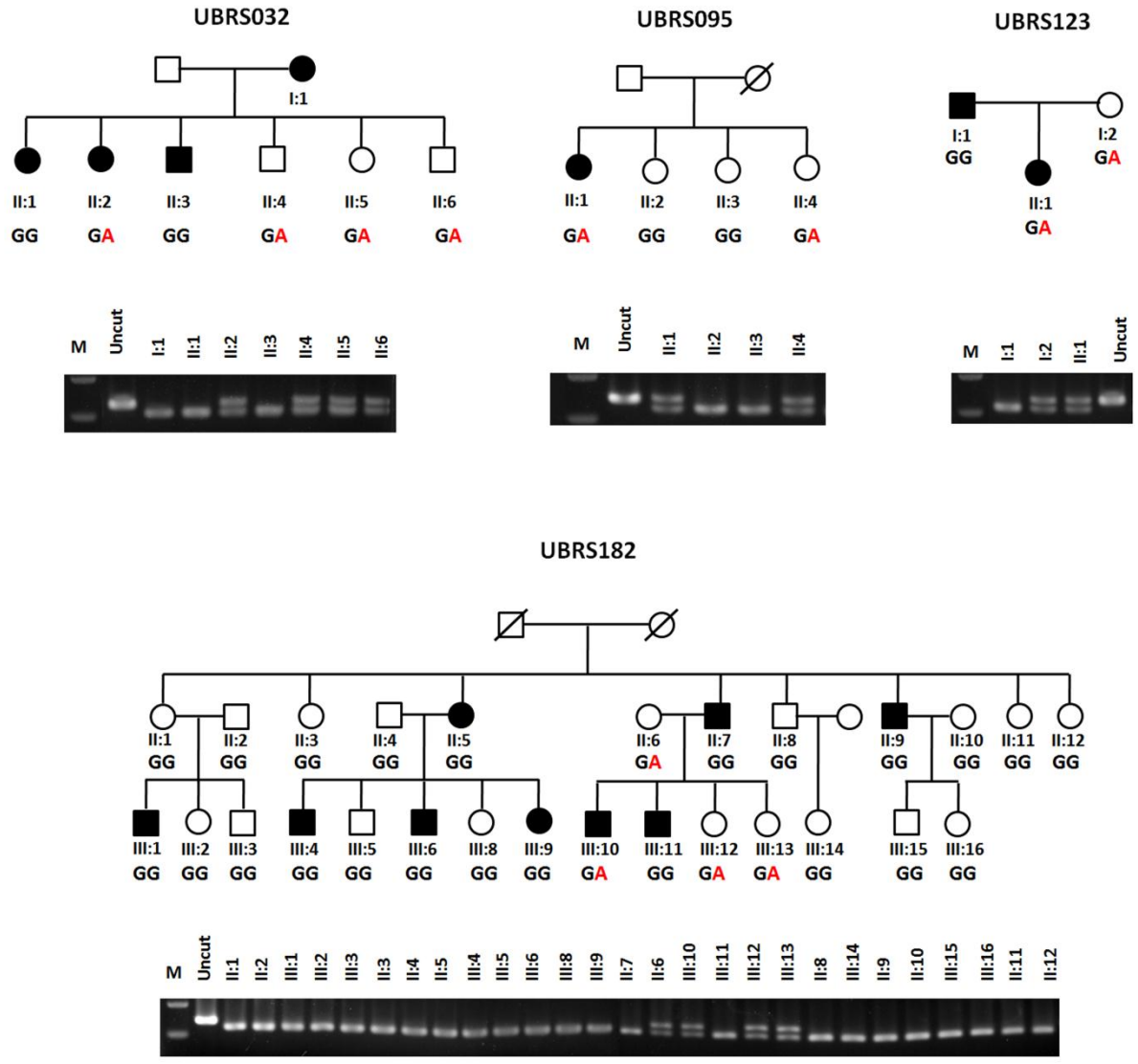


**Figure S2.** Segregation testing of KSD and *TTYH2* variation. p.M177I variation of *TTYH2* was genotyped by dCAPS technique in 4 affected families.

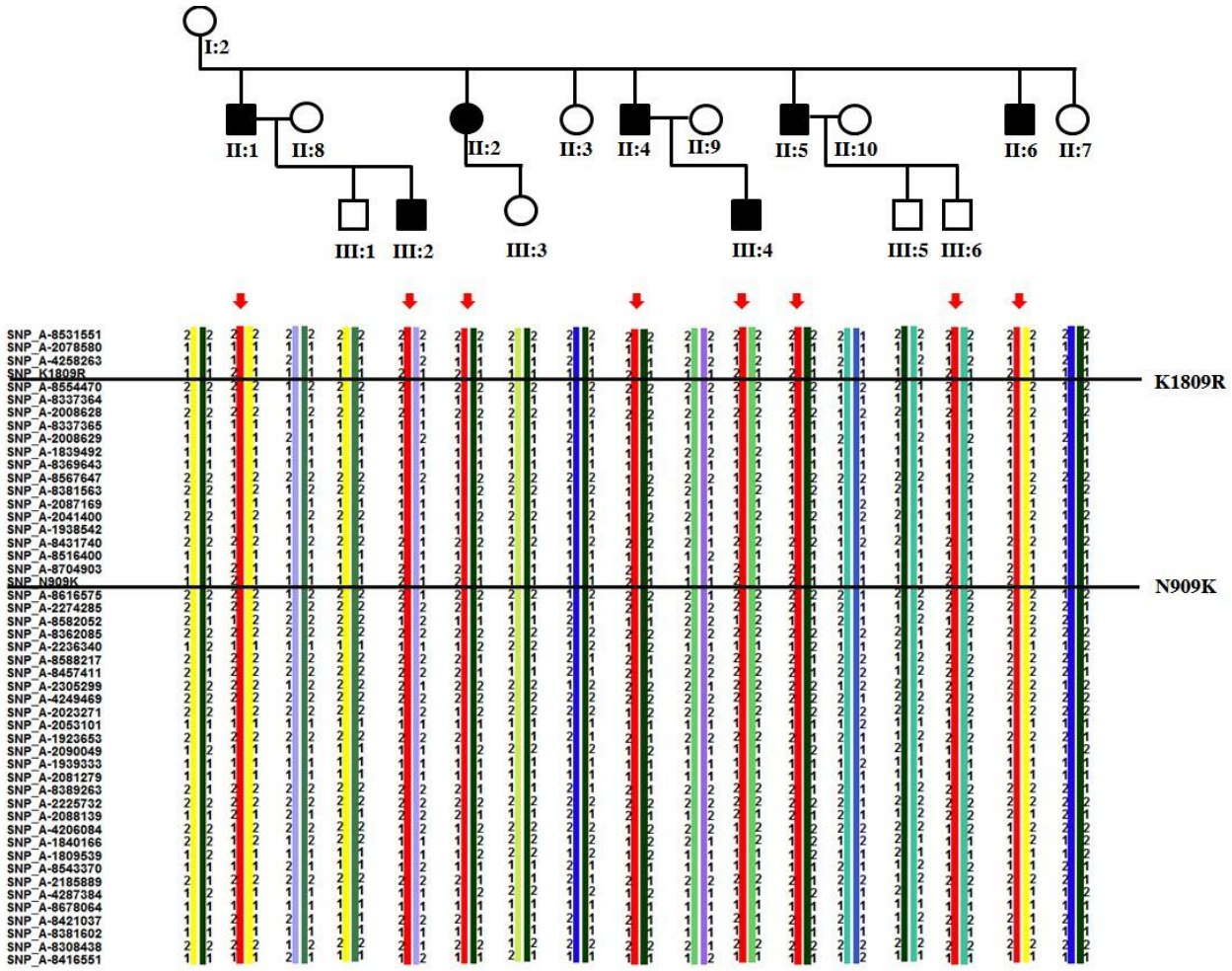


**Figure S3.** Haplotype analysis in the region of chromosome 3 where two variations in *SCN10A* (p.N909K and p.K1809R) and 49 single nucleotide polymorphisms (SNPs) were located, showing co-segregation of the haplotype in red color with KSD in the UBRS082 family.

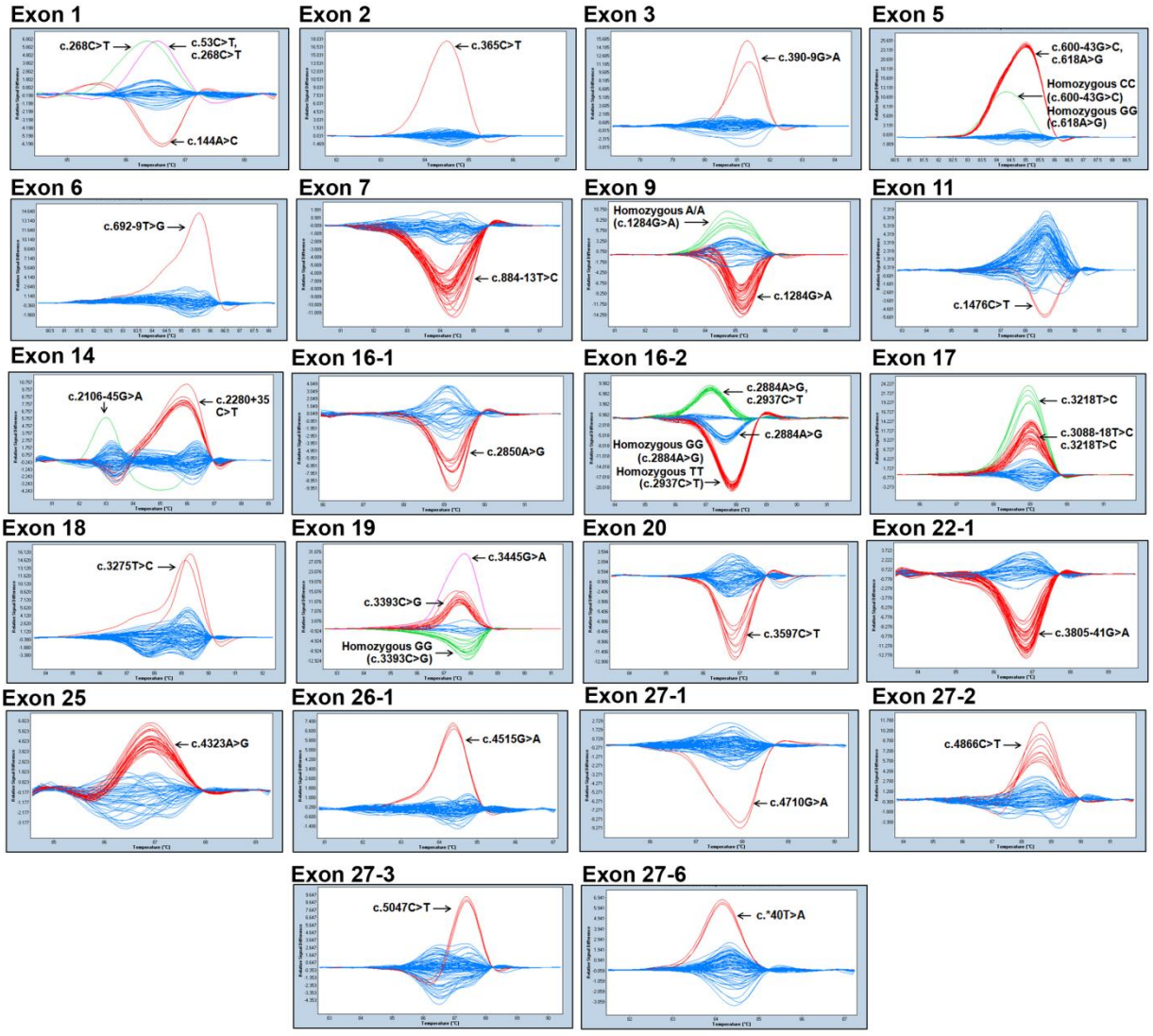


**Figure S4.** Screening of all 27 exons (including their exon-intron boundaries) of *SCN10A* in DNA samples from 180 patients with KSD by PCR-HRM method. Twenty-nine variations (1 novel and 28 reported variations) were identified, which were subsequently confirmed by Sanger DNA sequencing method.

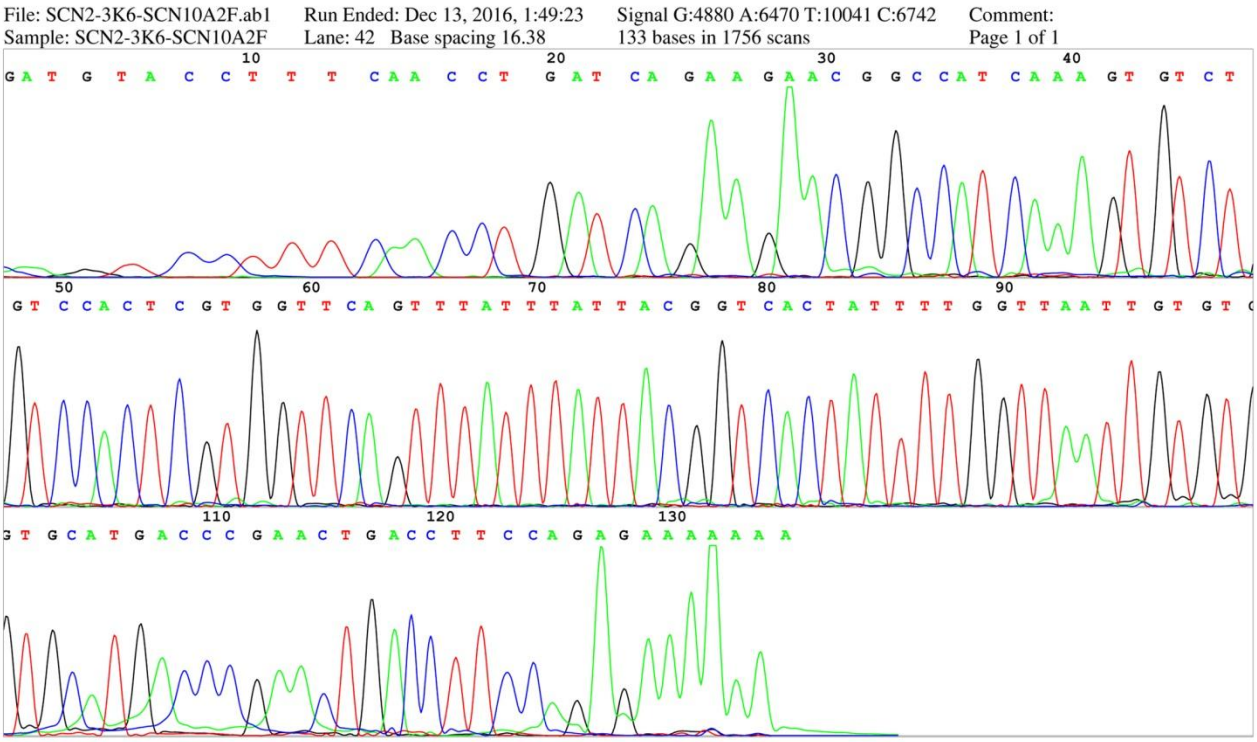


**Figure S5.** Sanger sequencing profile of *SCN10A* cDNA (exons 2-3), which was reversed transcribed from mRNA isolated from a human kidney tissue and amplified by polymerase chain reaction (PCR).

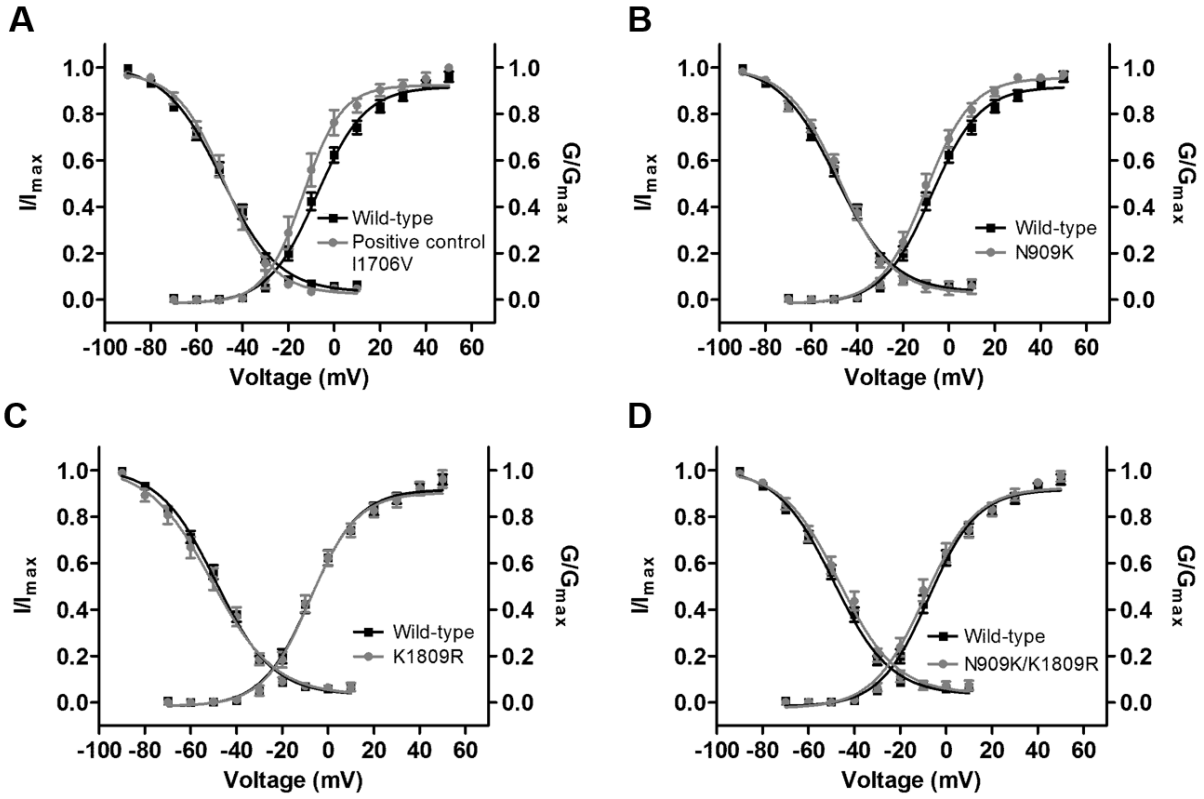


**Figure S6.** Comparison of the voltage dependence of activation ($G/G_{max}$, right curves and axis in each panel) and steady-state fast inactivation ($I/I_{max}$, left curves and axis) between wild-type and mutant $Na_V1.8$ channels; positive control (A), N909K (B), K1809R (C) and N909K/K1809R (D).

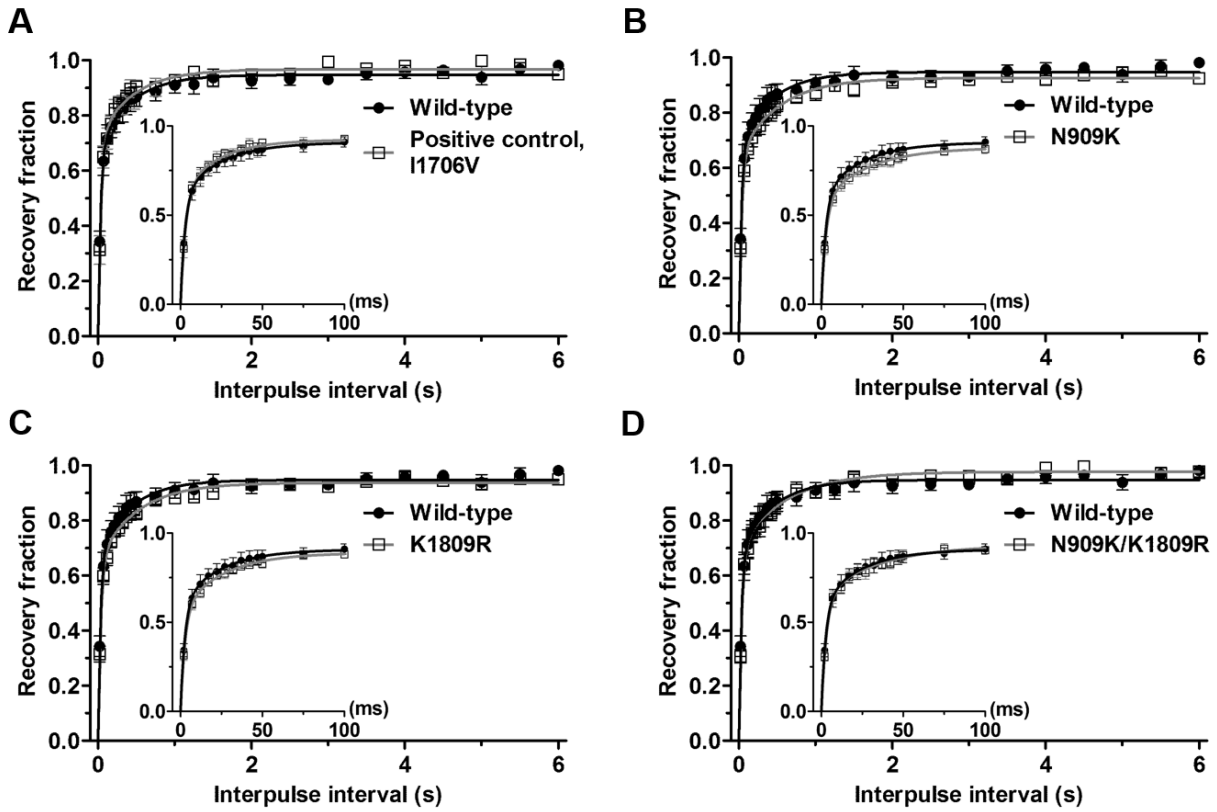


**Figure S7.** Time course of recovery from inactivation for wild-type and mutant $Na_V1.8$ channels at -80 mV. See Supplementary Table S8 for recovery time constant.

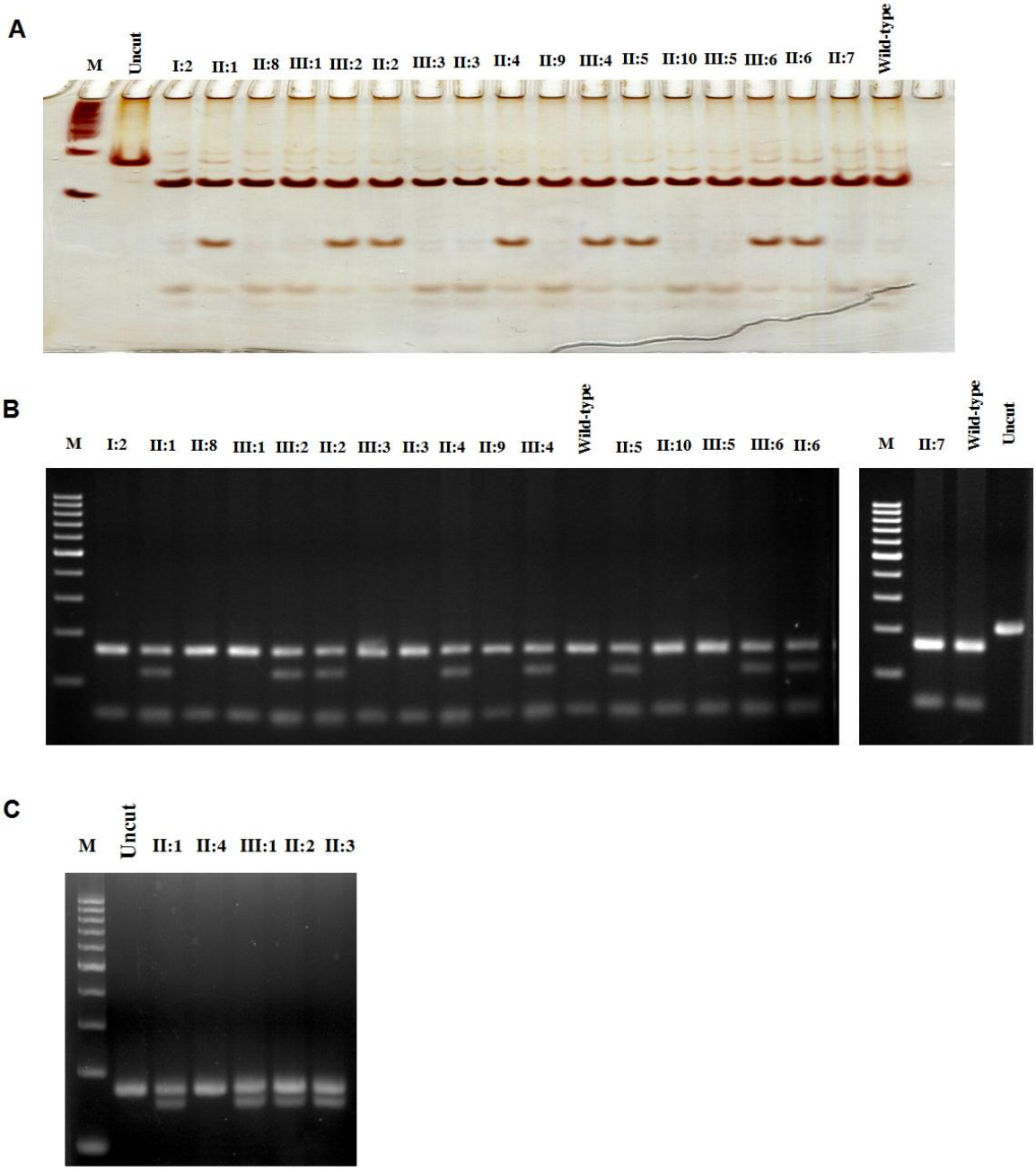


**Figure S8.** Segregation analysis of KSD and *SCN10A* variations in two affected families. (A) Co-segregation of KSD and *SCN10A* c.2727C>A and (B) c.5426A>G in the UBRS082 family. (C) Co-segregation of KSD and *SCN10A* c.3445G>A in the UBRS094 family.

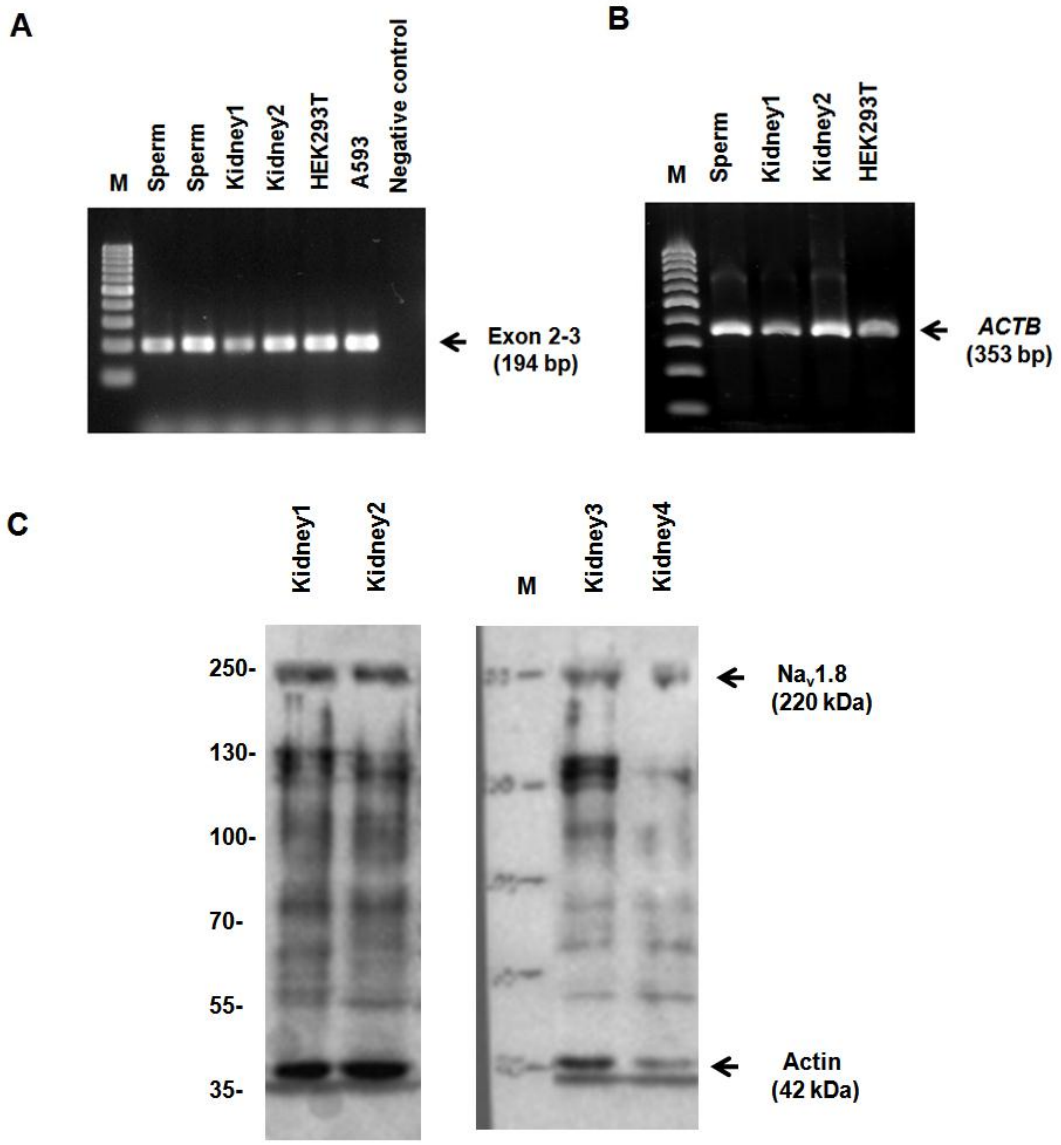


**Figure S9.** Expression of *SCN10A* mRNA and $Na_V1.8$ α subunit protein in human kidney tissues.

(A) Detection of *SCN10A* mRNA from human kidney tissues and cell line by RT-PCR method. *SCN10A* mRNA extracted from sperm was used as a positive control. A region of *SCN10A* mRNA covering exons 2-3 was analyzed, and (B) mRNA of a house-keeping gene– *ACTB* was used as an internal control. (C) Western-blot analysis showed $Na_V1.8$ α subunit of voltage-gated sodium channel expression in four human kidney tissue samples. Actin was used as loading control.

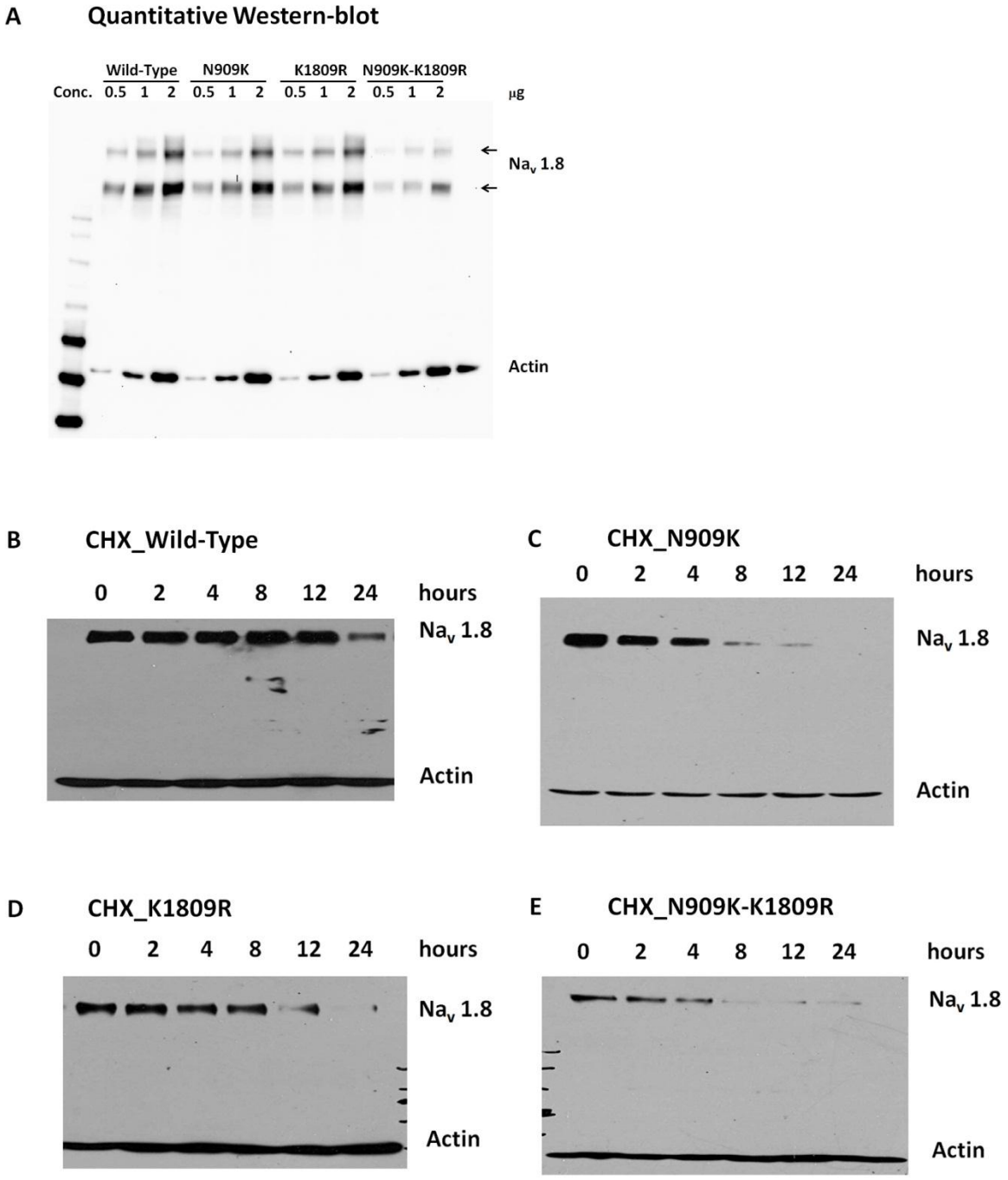


**Figure S10.** Effect of *SCN10A* mutations on the protein expression in transfected HEK293-1B cells.

(A) Semi-quantitative Western-blot analysis and quantitative representation of wild-type and mutant $Na_V1.8$ α subunit proteins and endogenously expressed actin. (B-E) Stabilities of wild-type and mutant $Na_V1.8$ α

subunit proteins in transfected HEK293-1B cells after treatment with 100 μg/ml of cycloheximide (CHX) for 0, 2, 4, 8, 12 and 24 hours. The wild-type and mutant proteins were quantified by GeneTools software version 4.03 (Syngene, UK).

**Supplementary tables**

**Table S1.** Results of linkage analyses showing the regions with Max LOD scores on chromosomes 3, 7 and 17.

| Chr. | Two-point parametric analysis | | | | Multi-point parametric analysis | | | | Non-parametric analysis | | | |
|---|---|---|---|---|---|---|---|---|---|---|---|---|
| | SNP 10K | | SNP 1M | | SNP 10K | | SNP 1M | | SNP 10K | | SNP 1M | |
| | Max LOD | Region(cM) | Max LOD | Region(cM) | Max LOD | Region(cM) | Max LOD | Region(cM) | Max LOD | Region(cM) | Max LOD | Region(cM) |
| 3 | 2.99 | 55.31 | 2.98 | 54.86-64.44 | 3.01 | 55.26-64.83 | 3.75 | 59.20-59.79 | 4.35 | 55.31-56.55, 59.98-65.17, 69.54-69.98, 78.48-83.21 | 4.35 | 59.83-60.64, 70.67-70.72, 84.03, 93.04, 95.84 |
| 7 | 2.99 | 122.09 | 3.01 | 120.47-122.24 | 3.01 | 120.61-122.39 | 2.98 | 120.31-123.83 | 4.34 | 118.44-122.37 | 4.75 | 123.24 |
| 17 | 1.79 | 113.61 | 3.01 | 110.39-125.65 | 2.89 | 113.62-114.24 | 2.98 | 109.77-126.19 | 4.01 | 113.62 | 4.75 | 26.93, 49.81, 116.99, 120.84-126.19 |

**Table S2.** Prediction of impacts of amino acid changes on protein structures and functions of 19 candidate variations by using 6 web based programs.

| Gene | Chromosome: position | SNP ID | Variations | | 1000G MAF | Predictions | | | | | |
|---|---|---|---|---|---|---|---|---|---|---|---|
| | | | DNA | Protein | | Polyphen | Vario watch | Mutation taster | SIFT | Mutation Assessor | LRT |
| *ZNF860* | 3: 32,032,397 | rs4955216 | c.1826G>T | p.R609L | 0.4307 | Benign | Low | Polymorphism | N/A | Neutral | N/A |
| *UBP1* | 3: 33,458,266 | rs3736563 | c.326A>G | p.N109S | 0.4790 | Benign | **High** | Polymorphism | Tolerated | Neutral | Neutral |
| *OXSR1* | 3: 38,271,881 | rs6599079 | c.911C>T | p.T304I | 0.1893 | Benign | Low | Polymorphism | Tolerated | Neutral | Neutral |
| *SLC22A14* | 3: 38,347,633 | rs34043027 | c.116G>A | p.R39H | 0.0751 | Benign | Low | Polymorphism | Tolerated | Low | Neutral |
| *SLC22A14* | 3: 38,347,851 | rs2073714 | c.334A>G | p.K112E | 0.0751 | Benign | **High** | Polymorphism | Tolerated | Neutral | Neutral |
| *SLC22A14* | 3: 38,355,225 | rs73064822 | c.1171G>A | p.V391I | 0.1669 | Benign | **High** | Polymorphism | Tolerated | Low | Neutral |
| *SLC22A14* | 3: 38,357,817 | rs2070492 | c.1535C>T | p.A512V | 0.1068 | **Possibly damaging** | **High** | Polymorphism | Tolerated | Low | Neutral |
| ***SCN10A*** | 3: 38,739,285 | rs561166361 | c.5426A>G | p.K1809R | 0.0002 | **Probably damaging** | **High** | **Disease causing** | **Damaging*** | **Medium** | **Deleterious** |
| *SCN10A* | 3: 38,768,300 | rs57326399 | c.2884A>G | p.I962V | 0.2107 | Benign | Low | Polymorphism | Tolerated | Neutral | Neutral |
| ***SCN10A*** | 3: 38,768,457 | rs567269429 | c.2727C>A | p.N909K | 0.0002 | Benign | **High** | **Disease causing** | Tolerated | **Medium** | Neutral |
| *SCN11A* | 3: 38,888,735 | rs72869687 | c.4826C>T | p.T1609I | 0.0693 | Benign | **High** | Polymorphism | Tolerated | Neutral | Neutral |
| *XIRP1* | 3: 39,225,752 | rs61736128 | c.5185G>C | p.V1729L | 0.1030 | Benign | Low | Polymorphism | Tolerated | Neutral | Unknown |
| ***XIRP1*** | 3: 39,226,436 | rs58805228 | c.4501G>A | p.V1501M | 0.1030 | **Possibly damaging** | **High** | Polymorphism | **Damaging** | **Medium** | Unknown |
| ***TTYH2*** | 17: 72,233,549 | rs371502920 | c.531G>A | p.M177I | 0.0008 | **Possibly damaging** | **High** | **Disease causing** | Tolerated | **Medium** | **Deleterious** |
| *LLGL2* | 17: 73,567,846 | rs1661715 | c.2275C>T | p.P759S | 0.3099 | **Possibly damaging** | Low | Polymorphism | Tolerated | Low | **Deleterious** |
| *LLGL2* | 17: 73,570,718 | rs1126939 | c.2981C>G | p.P994R | 0.3153 | Benign | Low | Polymorphism | **Damaging*** | N/A | N/A |
| *MGAT5B* | 17: 74,868,836 | rs732186 | c.5A>G | p.H2R | 0.0094 | Benign | **High** | Polymorphism | N/A | Neutral | N/A |
| *TMC6* | 17: 76,121,031 | rs34712518 | c.572G>A | p.G191D | 0.1038 | Benign | Low | Polymorphism | Tolerated | Low | Neutral |
| *DNAH17* | 17: 76,503,593 | rs9896398 | c.4531A>G | p.T1511A | 0.4215 | Benign | Low | Polymorphism | Tolerated | Neutral | N/A |

* Low confidence

**Table S3.** Genotyping and segregation analyses of selected four variations on *SCN10A*, *XIRP1*, and *TTYH2* in the UBRS082 family and in normal control subjects.

| Gene | Variation | Family (UBRS082) | | Control subjects (N=180) | |
|---|---|---|---|---|---|
| | | Segregation | LOD | No. of detected samples | Alleles frequency |
| *SCN10A* | N909K | Yes | 3.31 | 0 | 0 |
| *SCN10A* | K1809R | Yes | 3.31 | 0 | 0 |
| *XIRP1* | V1501M | Yes | 3.31 | 24 | 0.067 |
| *TTYH2* | M177I | Yes | 3.31 | 3 | 0.008 |

**Table S4.** A summary of *SCN10A* variations identified in additional 180 patients with KSD.

| No. of variations | SNP ID | Location | Nucleotide change | Amino acid change | Amino acid group change | No. of detected samples (n=180) | MAF |
|---|---|---|---|---|---|---|---|
| 1 | rs190176472 | Exon 1 | c.53C>T | P18L | Yes | 1 | 0.0028 |
| 2 | rs368338265 | Exon 1 | c.144A>C | E48D | No | 2 | 0.0056 |
| 3 | rs144270136 | Exon 1 | c.268C>T | R90W | Yes | 2 | 0.0056 |
| 4 | rs142884499 | Exon 2 | c.365C>T | T122M | Yes | 1 | 0.0028 |
| 5 | rs370917734 | Intron 2 | c.390-9G>A | - | - | 2 | 0.0056 |
| 6 | rs73826327 | Intron 4 | c.600-43G>C | - | - | 39 | 0.1250 |
| 7 | rs74717885 | Exon 5 | c.618A>G | I206M | No | 39 | 0.1250 |
| 8 | Novel | Intron 5 | c.692-9T>G | - | - | 1 | 0.0028 |
| 9 | rs7641844 | Intron 6 | c.884-13T>C | - | - | 108 | 0.3000 |
| 10 | rs62244070 | Exon 9 | c.1284G>A | E428E | No | 58 | 0.1833 |
| 11 | rs7617919 | Exon 11 | c.1476C>T | L492L | No | 3 | 0.0083 |
| 12 | rs544900253 | Intron 13 | c.2106-45G>A | - | - | 1 | 0.0028 |
| 13 | rs9830687 | Intron 14 | c.2280+35C>T | - | - | 28 | 0.0778 |
| 14 | rs7374804 | Exon 16 | c.2850A>G | K950K | No | 23 | 0.0638 |
| 15 | rs57326399 | Exon 16 | c.2884A>G | I962V | No | 113 | 0.4250 |
| 16 | rs59468016 | Exon 16 | c.2937C>T | G979G | No | 85 | 0.2361 |
| 17 | rs11129804 | Intron 16 | c.3088-18T>C | - | - | 80 | 0.2222 |
| 18 | rs6795970 | Exon 17 | c.3218T>C | V1073A | Yes | 88 | 0.2444 |
| 19 | rs12632942 | Exon 18 | c.3275T>C | L1092P | No | 5 | 0.0167 |
| 20 | rs6771157 | Exon 19 | c.3393C>G | T1131T | No | 135 | 0.4667 |
| 21 | rs560631745 | Exon 19 | c.3445G>A | V1149M | No | 1 | 0.0028 |
| 22 | rs758184076 | Exon 20 | c.3597C>T | F1199F | No | 14 | 0.0389 |
| 23 | rs6781740 | Intron 21 | c.3805-41G>A | - | - | 77 | 0.2139 |
| 24 | rs6790627 | Exon 25 | c.4323A>G | K1441K | No | 56 | 0.1556 |
| 25 | rs191624001 | Exon 26 | c.4515G>A | T1505T | No | 6 | 0.0167 |
| 26 | rs78425180 | Exon 27 | c.4710G>A | T1570T | No | 10 | 0.0278 |
| 27 | rs6599242 | Exon 27 | c.4866C>T***** | S1622S | No | 17 | 0.0472 |
| 28 | rs146999807 | Exon 27 | c.5047C>T | P1683S | No | 3 | 0.0083 |
| 29 | rs142813340 | 3’ UTR | c.*40T>A | - | - | 12 | 0.0333 |

*****: T is reported as major allele in SNP database, n: number of patients with nephrolithiasis, MAF: Minor allele frequency.

**Table S5.** Prediction of impacts of amino acid changes on the protein structure and function of $Na_V1.8$ α subunit resulting from the identified variations in exons of *SCN10A* by using 6 web-based programs.

| SNP ID | Location | Nucleotide change | Amino acid change | 1000G MAF | Function Prediction | | | | | |
|---|---|---|---|---|---|---|---|---|---|---|
| | | | | | Polyphen2 | Vario Watch | MutationTaster | SIFT | MutationAssessor | LRT |
| rs190176472 | Exon 1 | c.53C>T | P18L | 0.0006 | **Probably damaging** | Medium | **Disease causing** | Tolerated | Low | Neutral |
| rs368338265 | Exon 1 | c.144A>C | E48D | N/A | Benign | Low | Polymorphism | Tolerated | Low | Neutral |
| rs144270136 | Exon 1 | c.268C>T | R90W | 0.0054 | **Probably damaging** | **High** | **Disease causing** | **Damaging** | **Medium** | Neutral |
| rs142884499 | Exon 2 | c.365C>T | T122M | 0.0004 | Benign | **High** | Polymorphism | **Damaging** | **Medium** | Neutral |
| rs74717885 | Exon 5 | c.618A>G | I206M | 0.0419 | Benign | Low | Polymorphism | Tolerated | Neutral | Neutral |
| rs62244070 | Exon 9 | c.1284G>A | E428E | 0.2075 | Benign | Low | Polymorphism | Tolerated | N/A | N/A |
| rs7617919 | Exon 11 | c.1476C>T | L492L | 0.2077 | Benign | Low | Polymorphism | Tolerated | N/A | N/A |
| rs7374804 | Exon 16 | c.2850A>G | K950K | 0.1360 | Benign | Low | Polymorphism | Tolerated | N/A | N/A |
| rs57326399 | Exon 16 | c.2884A>G | I962V | 0.2107 | Benign | Low | Polymorphism | Tolerated | Neutral | Neutral |
| rs59468016 | Exon 16 | c.2937C>T | G979G | 0.1905 | Benign | Low | Polymorphism | Tolerated | N/A | N/A |
| rs6795970 | Exon 17 | c.3218T>C | V1073A | 0.2420 | Benign | Low | Polymorphism | Tolerated | Neutral | Neutral |
| rs12632942 | Exon 18 | c.3275T>C | L1092P | 0.2196 | Benign | Low | Polymorphism | Tolerated | N/A | N/A |
| rs6771157 | Exon 19 | c.3393C>G | T1131T | 0.2196 | Benign | Low | Polymorphism | Tolerated | N/A | N/A |
| rs560631745 | Exon 19 | c.3445G>A | V1149M | 0.0002 | **Probably damaging** | **High** | **Disease causing** | **Damaging** | **Medium** | **Deleterious** |
| rs758184076 | Exon 20 | c.3597C>T | F1199F | N/A | Benign | Low | Polymorphism | Tolerated | N/A | N/A |
| rs6790627 | Exon 25 | c.4323A>G | K1441K | 0.2424 | Benign | Low | Polymorphism | Tolerated | N/A | N/A |
| rs191624001 | Exon 26 | c.4515G>A | T1505T | 0.0030 | Benign | Low | Polymorphism | Tolerated | N/A | N/A |
| rs78425180 | Exon 27 | c.4710G>A | T1570T | 0.0579 | Benign | Low | Polymorphism | Tolerated | N/A | N/A |
| rs6599242 | Exon 27 | c.4866C>T | S1622S | 0.0753 | Benign | Low | Polymorphism | Tolerated | N/A | N/A |
| rs146999807 | Exon 27 | c.5047C>T | P1683S | 0.0024 | Benign | Low | Polymorphism | Tolerated | Low | Neutral |

**Table S6.** Some clinical and laboratory data of the members of the UBRS094 family.

| Sample No. | Gender | Age | Age of Onset* | KUB result | Site/Side of stone | No. of stone | Treatment | Urine pH | Other Symptoms | | | | Diagnosis |
|---|---|---|---|---|---|---|---|---|---|---|---|---|---|
| | | | | | | | | | Dysuria | Hematuria | Pass Stone | Turbid Urine | |
| II:1 | Male | 56 | 40 | Negative | N/A | N/A | No | 5.3 | Yes | Yes | Yes | Yes | renal stone (strong clinical history[1]) |
| II:2 | Female | 34 | 24 | Positive | Renal/ Both | 4 | Surgery | 6.7 | Yes | Yes | No | Yes | renal stone (KUB[2]) |
| II:3 | Female | 33 | 30 | Positive | Renal/Left | 1 | No | 5.8 | Yes | Yes | No | No | renal stone (KUB) |
| III:1 | Female | 26 | 25 | Positive | Renal/Left | 1 | No | 5.9 | Yes | No | No | Yes | renal stone (KUB) |
| II:4 | Female | 56 | - | Negative | No | - | No | 5.0 | No | No | No | No | no stone |

[1] The patient had strong clinical history as justified from the presence of several symptoms associated with kidney stone, especially hematuria and stone passage.

[2] The patient had positive results of kidney–ureter–bladder (KUB) radiography.

[*] Age at the onset of kidney stone disease.

**Table S7.** Average time constant of inactivation at 0 mV and persistent currents associated to wild-type and mutant $Na_V1.8$ channels.

| $Na_V1.8$ | Time constant of inactivation (0 mV) | | Persistent currents (0 mV) | |
|---|---|---|---|---|
| | ms | n | % of I peak | n |
| Wild-type | 4.83 ± 0.79 | 23 | 8.62 ± 1.04 | 23 |
| I1706V | 2.99 ± 0.45 | 12 | 2.24 ± 1.16* | 12 |
| N909K | 4.68 ± 0.59 | 22 | 3.61 ± 1.50* | 22 |
| K1809R | 7.49 ± 0.72** | 24 | 8.45 ± 1.82 | 23 |
| N909K/ K1809R | 6.12 ± 0.89 | 24 | 10.72 ± 1.62 | 24 |

Time constants were obtained by fitting decaying currents with a single-exponential function. Persistent currents were the mean current between 93-98 ms. *$p < 0.05$, **$p < 0.01$ vs wild-type (unpaired t-test).

**Table S8.** Average recovery time constant (at -80 mV) for fast and slow inactivation of wild-type and mutant $Na_V1.8$ channels.

| $Na_V1.8$ | Recovery time constant (ms) | | n |
|---|---|---|---|
| | Fast component | Slow component | |
| Wild-type | 3.48 ± 0.36 | 82.35 ± 25.62 | 11 |
| I1706V | 4.84 ± 1.02 | 110.2 ± 30.61 | 10 |
| N909K | 4.00 ± 0.73 | 63.91 ± 10.01 | 16 |
| K1809R | 3.71 ± 0.50 | 70.38 ± 16.15 | 16 |
| N909K/ K1809R | 3.82 ± 0.49 | 89.67 ± 22.82 | 11 |

No significant difference was found between wild-type and mutant $Na_V1.8$ channels.

**Table S9.** Some characteristics of the patients with kidney stone disease (KSD) and normal control subjects.

| Characteristics | Patients (n) | % | Controls (n) | % |
|---|---|---|---|---|
| **Gender** | | | | |
| Female | 77 | 42.78 | 81 | 45.00 |
| Male | 103 | 57.22 | 99 | 55.00 |
| **Age** | | | | |
| Mean (years) | 44.1 ± 12.8 | - | 44.3 ± 12.5 | - |
| Range (years) | 22-73 | - | 21-75 | - |
| **Familial history** | | | | |
| Yes | 128 | 71.11 | - | - |
| No | 52 | 28.89 | - | - |
| **Stone number** | | | | |
| Single | 50 | 27.78 | - | - |
| Multiple | 120 | 66.67 | - | - |
| Unknown | 10 | 5.55 | - | - |
| **Position of stone** | | | | |
| Kidney | 163 | 90.55 | - | - |
| Ureter | 5 | 2.78 | - | - |
| Kidney and ureter | 12 | 6.67 | - | - |

**Table S10.** PCR primers for genotyping 4 genetic variations in *SCN10A*, *SCN10A*, *XIRP1*, and *TTYH2* genes in the members of UBRS082 family and 180 normal control subjects.

| Gene | Variation | Nucleotide sequence (5'→3') | Number of nucleotides | Tm (°C) | Product size (bp) |
|---|---|---|---|---|---|
| *SCN10A* | N909K | TGGGGCTCAGCTTAGAGATTGA | 22 | 63.5 | |
| | | ATCCGTGCCAGGGCCACCTGCCG | 23 | 76.9 | 162 |
| *SCN10A* | K1809R | CCAAAACCCAATCGAAATATAC | 22 | 57.5 | |
| | | AGAGTGGTTGCTATTGGTTCAT | 22 | 57.8 | 206 |
| *XIRP1* | V1501M | GCCCTGCGGAGGCTCTTTGTGGCC | 24 | 77.6 | |
| | | TTGCCAAGGTCTGTTCCTTCAG | 22 | 63.8 | 160 |
| *TTYH2* | M177I | AAGGTGGACCTAGAGCAGCA | 20 | 60.0 | |
| | | GAGAGCTGAACAACAACGC | 19 | 57.1 | 119 |

**Table S11.** PCR primers for amplifications of all exons of *SCN10A* for screening and sequencing of its genetics variations.

| Fragments No. | Region | Primer name | Nucleotide sequence (5'→3') | Number of nucleotides | Tm (°C) | Product size (bp) |
|---|---|---|---|---|---|---|
| F1 | Exon 1 | F1F | CAGTGGGCAAGCTGTCAC | 18 | 58.9 | 436 |
| | | F1R | AGGGCCAAGGAGGACTTTCT | 20 | 61.4 | |
| F2 | Exon 2 | F2F | CCTGAGATAATGCCTCTCATGT | 22 | 58.3 | 275 |
| | | F2R | GTACTGGACACAGTAGGCAAGG | 22 | 58.8 | |
| F3 | Exon 3 | F3F | GTAATCATTCAGCATCAAGGTG | 22 | 57.2 | 240 |
| | | F3R | AAGACAAAGACTGCCAAGTGAA | 22 | 59.0 | |
| F4 | Exon 4 | F4F | GGTCATCCCTCCCTCCTG | 18 | 60.4 | 283 |
| | | F4R | CCCTGTCTCCTACCCACCA | 19 | 60.9 | |
| F5 | Exon 5 | F5F | CCCAGGTTATCCTTATTTATGCT | 23 | 57.7 | 265 |
| | | F5R | TCTTTGCCCTGGAACCTTAC | 20 | 59.1 | |
| F6 | Exon 6 | F6F | AGAGATGAAGGAGGATGGCTA | 21 | 57.9 | 365 |
| | | F6R | ACACAGGGGCTCCATATCC | 19 | 59.7 | |
| F7 | Exon 7 | F7F | TCACTTTGGAAGACTTGGGAAT | 22 | 59.9 | 240 |
| | | F7R | GCCCATAATATGCCAAGGAC | 20 | 59.2 | |
| F8 | Exon 8 | F8F | AAGTGTCCAAGATCATCCTGCT | 22 | 60.1 | 364 |
| | | F8R | CTCCTCCAGGAAAAGCACAG | 20 | 59.9 | |
| F9 | Exon 9 | F9F | TCCTGGAGGAGGCTGACTT | 19 | 59.3 | 367 |
| | | F9R | ACGGTGCCCTAATTGAAGTG | 20 | 60.5 | |
| F10 | Exon 10 | F10F | CATGTCTGGGGGACACATTC | 20 | 61.2 | 322 |
| | | F10R | CCTCTTCCCACTCCAACTCA | 20 | 60.2 | |
| F11 | Exon 11 | F11F | AGAGGGAAGTGTTGGGCTCT | 20 | 60.5 | 449 |
| | | F11R | TTGGTGATACTCAGGCTTCTTG | 22 | 61.3 | |
| F12 | Exon 12 | F12F | TGGCCAATAAGAGGCTGAAT | 20 | 59.6 | 266 |
| | | F12R | TTGCTTCTGCTGCTCACATG | 20 | 61.3 | |
| F13 | Exon 13 | F13F | AGAGGATGACCGCAGAATTG | 20 | 60.9 | 385 |
| | | F13R | GAACTGCACCCTGCCATC | 18 | 58.9 | |
| F14 | Exon 14 | F14F | CCTCAGGAGCCCACAGATAA | 20 | 60.2 | 387 |
| | | F14R | CCCAGAGCACAGTGTCTTCC | 20 | 60.8 | |

**Table S11.** (Continued).

| Fragments No. | Region | Primer name | Nucleotide sequence (5'→3') | Number of nucleotides | Tm (°C) | Product size (bp) |
|---|---|---|---|---|---|---|
| F15/1 | Exon 15 | F15/1F | TCTTTGGTTTCCAGGCAAAA | 20 | 60.6 | 310 |
| | | F15/1R | TGGAAGAAGTCGTGCATGTG | 20 | 60.9 | |
| F15/2 | Exon 15 | F15/2F | GGGAAAACTACCGTAACAACC | 21 | 57.3 | 309 |
| | | F15/2R | TCTGGGCATAAAAATGCAGA | 20 | 59.2 | |
| F16/1 | Exon 16 | F16/1F | CTAACCCGGTAGGCCAATGT | 20 | 61.1 | 326 |
| | | F16/1R | GTTGGCAGCAATGTGGTTC | 19 | 60.1 | |
| F16/2 | Exon 16 | F16/2F | CCCACTCTCCAGCTCCAAG | 19 | 60.9 | 323 |
| | | F16/2R | TCCTCTGCATTTCCCTTTTG | 20 | 60.1 | |
| F17 | Exon 17 | F17F | TGATGTGCAAGATCCCTTCA | 20 | 60.2 | 298 |
| | | F17R | ACCCTCCAGCCTCTACCAG | 19 | 59.2 | |
| F18 | Exon 18 | F18F | CAAACATGGGTGCAGTTGAA | 20 | 60.5 | 300 |
| | | F18R | TGGATCCCAGGTGAGTGTTC | 20 | 60.9 | |
| F19 | Exon 19 | F19F | TGGGTTTCCTAGCAGAATGG | 20 | 60.1 | 339 |
| | | F19R | AGAACCCACTGATGCAGCTC | 20 | 60.4 | |
| F20 | Exon 20 | F20F | GCTGGGTCCTTCCCTATCAG | 20 | 60.9 | 341 |
| | | F20R | GGTCTCTGAGCTTCCTTTGC | 20 | 59.1 | |
| F21 | Exon 21 | F21F | GGGAGTTCCTGTCTCCTTCC | 20 | 60.1 | 240 |
| | | F21R | GTGCCTGGCCAGATGAGA | 18 | 60.9 | |
| F22/1 | Exon 22 | F22/1F | CTCATGAAGCAGCCTGAATG | 20 | 59.5 | 311 |
| | | F22/1R | CTGCCAGTGGAGTTTTGAAT | 20 | 57.8 | |
| F22/2 | Exon 22 | F22/2F | TGTACCTTTGTCGATTGTGAAT | 22 | 57.1 | 225 |
| | | F22/2R | GCAAAGTCCCCACATAGCAT | 20 | 59.9 | |
| F23 | Exon 23 | F23F | CTCTCACTGGGCCACCAT | 18 | 59.6 | 230 |
| | | F23R | ACCAGGGTCATCGTCACTTC | 20 | 59.9 | |
| F24 | Exon 24 | F24F | TGTCTTAGGCTTGGCTTTCA | 20 | 58.6 | 290 |
| | | F24R | AGAGCTGGGCAGGGAACA | 18 | 61.9 | |
| F25 | Exon 25 | F25F | CCTTTCTCTCCTGCCTGTTC | 20 | 59.0 | 248 |
| | | F25R | AGGCATAGACTGTCATGTTGGA | 22 | 59.6 | |

**Table S11.** (Continued).

| Fragments No. | Region | Primer name | Nucleotide sequence (5'→3') | Number of nucleotides | Tm (°C) | Product size (bp) |
|---|---|---|---|---|---|---|
| F26/1 | Exon 26 | F26/1F | TGTGGAGTGTGATGGAGACAA | 21 | 60.1 | 285 |
| | | F26/1R | GACACATTCGCCTGTGAAGA | 20 | 59.8 | |
| F26/2 | Exon 26 | F26/2F | AGACGAAAATTCTGGGCAAA | 20 | 59.6 | 236 |
| | | F26/2R | TTGGTTGGTTATTTCCTTGG | 20 | 57.4 | |
| F27/1 | Exon 27 | F27/1F | CCAAGCAAAGCAGAGTGTCA | 20 | 60.1 | 269 |
| | | F27/1R | AACAGCCCGATGTTGAAGAG | 20 | 60.2 | |
| F27/2 | Exon 27 | F27/2F | ATCCGCACACTGCTCTTTG | 19 | 60.0 | 272 |
| | | F27/2R | GGCAGATTGGGGTCACAGTA | 20 | 60.9 | |
| F27/3 | Exon 27 | F27/3F | AGCCCCATCCTCAACACA | 18 | 60.1 | 297 |
| | | F27/3R | GTCCGAGAGAGCAGAAAAGG | 20 | 59.1 | |
| F27/4 | Exon 27 | F27/4F | CCCTGAGTGAGGACGACTTT | 20 | 59.3 | 334 |
| | | F27/4R | AGAGTGGTTGCTATTGGTTCA | 21 | 57.4 | |
| F27/5 | Exon 27 | F27/5F | TGGAGGAGAAGTTTATGGCAAC | 22 | 60.5 | 293 |
| | | F27/5R | CTCATAGGACGGTGGGAATG | 20 | 60.3 | |
| F27/6 | Exon 27 | F27/6F | CCCAGACAAATCTGAAACTGC | 21 | 59.7 | 247 |
| | | F27/6R | TGTAGCTGGGTGTGATCTGC | 20 | 59.9 | |

**Table S12.** PCR primers for analysis of *SCN10A* expression.

| Gene | Nucleotide sequence (5'→3') | Number of nucleotides | Tm (°C) | Product size (bp) |
|---|---|---|---|---|
| *SCN10A* exon 2-3 | CATTTATGGTGCTGAACAAAGG | 22 | 52.7 | |
| | TTTCTCTGGAAGGTCAGTTCG | 21 | 54.2 | 194 |
| *ACTB* | GCTCGTCGTCGACAACGGCTC | 21 | 62.3 | |
| | CAAACATGATCTGGGTCATCTTCTC | 25 | 55.6 | 353 |

**Supplementary methods**

**Genome-wide linkage analysis**

Genome-wide linkage analysis was performed in a selected family (UBRS082) with a maximal ELOD of 3.31, containing 17 members (7 affected and 10 unaffected), by using either SNP 10K array (Human Mapping 10K 2.0; Affymetrix, USA) or SNP 1M array (Genome-Wide Human SNP Array 6.0; Affymetrix, USA) for SNP genotyping of the DNA samples from all 17 members.

The experimental steps for SNP genotyping by SNP 10K array (Human Mapping 10K 2.0) were conducted by following the manufacturer's instruction. To obtain higher genomic coverage, SNP genotyping was repeated by using SNP 1M array (Genome-Wide Human SNP Array 6.0). The DNA samples from all 17 members were sent to the Functional Genomics Shared Resource (Vanderbilt University, Tennessee, USA) for SNP genotyping. The SNP genotyping data from both arrays were analyzed by easyLINKAGE software[1] compiling many useful types of software for linkage analysis including FastLink, SuperLink, SPLink, GeneHunter, Merlin, Simwalk2, PedCheck and FastSLink. The analyses were carried out by both parametric and non-parametric modes, and in both two-point and multi-point methods. Regions with significant (LOD >2.80) or highest LOD scores were selected for further investigations.

**Exome sequencing**

Two DNA samples of affected members (II:5 and II:6) and one unaffected member (II:7) were taken for exome capturing by IlluminaTruSeqExome Enrichment kits (Illumina,California, USA) and sequencing by IlluminaHiSeq 2000 (Illumina,California, USA). The DNA samples were sent to the Axeq Asia (Seoul, South Korea), for the exome capturing and sequencing steps by following the Illumina protocols. The reads were mapped against UCSC hg19 by Burrows-Wheeler Aligner and variations (SNPs and Indels) and were detected by Sequence Alignment/Map.

Genetic variations acquired from exome sequencing data in the chromosomal regions with high LOD scores (>2.80) were taken for the analysis. The variations outside exonic regions were initially excluded as they were likely to be non-disease causing polymorphisms. Since KSD in the UBRS082 family was inherited as autosomal dominant mode, the genetic variations that were shared in the two affected family members but not observed in the unaffected family member were selected for further analyses. The variations in exons that caused non-synonymous changes, stop gain/loss variants or short insertions or deletions (indels) were considered for further analysis.

The possible impacts of amino acid changes on structure and function of protein were predicted by using 6 web-based programs: Polymorphism Phenotyping v2 (PolyPhen-2),[2] VarioWatch,[3] MutationTaster,[4] Sorting Intolerant From Tolerant (SIFT),[5] MutationAssessor,[6] and Likelihood Ratio Test (LRT).[7] The impact of exon-intron boundaries on mRNA splicing process was evaluated using ESEfinder 2.0.[8] Multiple amino acid sequence alignment of $Na_V1.8$ α subunit of voltage-gated sodium channel from human, chimpanzee, orangutans, gibbon, dog, cow, mouse, rat, anole and chicken were carried out by using ClustalW2 program.

**Genotyping of genetic variations in family members and normal control subjects**

Nucleotide sequences of the genes of interest were acquired from the GenBank database for designing polymerase chain reaction (PCR) primers (Table S10). The specific primer-pairs generated amplicons with the sizes between 119 and 206 bp, covering genetic variations of interest for genotyping DNA samples of family members and normal control subjects by using PCR-high resolution melting (PCR-HRM) analysis[9,10] and either PCR-restriction fragment length polymorphism (PCR-RFLP) or derived cleaved amplified polymorphic sequences (dCAPS) method.[11] The genetic variations that were observed by these genotyping methods in all DNA samples were confirmed by Sanger DNA sequencing.

**Screening of genetic variations in *SCN10A* by PCR-HRM method**

The whole nucleotide sequence of *SCN10A* was obtained from the GenBank database. Thirty-six pairs of PCR primers covering 27 exons and their exon-intron boundaries were designed (Table S11) and synthesized. Genetic variations in *SCN10A* in DNA samples of the patients with KSD were screened by PCR-HRM method by using a LightCycler 480 II machine (Roche Diagnostics International Ltd., Rotkreuz, Switzerland). The PCR mixture contained Resolight dye (Roche Diagnostics GmbH, Mannheim, Germany) for detection of PCR products and for analysis of their melting curves. The melting curve was normalized for temperature-shifted difference plot by Gene Scanning 1.5.0 software (Roche Diagnostics International Ltd., Rotkreuz, Switzerland). The PCR products with melting profile different from the normal pattern were further analyzed by Sanger DNA sequencing.

**DNA sequencing**

PCR product for DNA sequencing was prepared in PCR reaction volume of 50 μL containing 200 ng genomic DNA in 1x reaction buffer, 0.5 μM of each primer, 0.2 mM dNTP, 2.0 mM $MgCl_2$ and 1.25 unit of DNA polymerase (HS Prime *Taq* DNA polymerase, GENET BIO Inc., Daejeon, South Korea) by using a TProfessional standard thermocycler (Biometra GmbH, Goettingen, Germany). The PCR product was purified before processing for direct DNA sequencing by the Sanger method. The sequencing reaction was carried out by using BigDye™ Terminator, which was conducted by a service provider - First BASE Laboratories Sdn Bhd (Selangor, Malaysia). The sequencing data was analyzed by comparing with a reference nucleotide sequence by multiple sequence alignment using ClustalW2 program.

**Human kidney tissues**

The study using human kidney tissues was approved by the Human Research Ethics Committee, Siriraj Institutional Review Board, Mahidol University. Human fresh frozen tissues from the patients without KSD were obtained from remaining biopsy specimens from the Department of Pathology, Faculty of

Medicine Siriraj Hospital, Mahidol University. These tissues were used for the studies of *SCN10A* mRNA expression by reverse transcription and polymerase chain reaction (RT-PCR) method, and its encoded protein ($Na_V1.8$ α subunit of voltage-gated sodium channel) expression by Western-blot analysis, immunohistochemistry and double immunofluorescence staining.

**Reverse transcription and polymerase chain reaction (RT-PCR)**

Total RNAs were extracted from human fresh frozen kidney tissues, human sperm, and HEK293T cells by Trizol reagent (Invitrogen, Carlsbad, CA, USA), following the manufacturer's protocol. RNA was then reverse-transcribed into cDNA by using oligo dT and SuperScript™ III First-Strand synthesis system (Invitrogen, Carlsbad, CA, USA). *SCN10A* cDNA was examined by PCR amplifications of a region covering exons 2-3 of *SCN10A*, and *ACTB* cDNA was amplified to serve as an internal control. The primer sequences are shown in Table S12. The RT-PCR products from kidney tissues were further analyzed by Sanger DNA sequencing.

**Western-blot analysis**

Proteins were extracted from human kidney tissue sections (20-μm thick) in 2x SDS buffer or from transfected cells in RIPA. Ten μl of human kidney tissue protein or 15 μl of protein from transfected cells of each sample was separated by SDS-polyacrylamide gel electrophoresis (PAGE). After electrophoresis, the proteins were transferred onto a nitrocellulose membrane by following a standard protocol. The membrane was blocked with 5% skim milk in TBST solution and incubated with rabbit anti-human $Na_V1.8$ α subunit of voltage-gated sodium channel (Abcam, Cambridge, UK) or mouse anti-SCN1B (Abcam, Cambridge, UK), followed by incubation with swine anti-rabbit antibody conjugated-horseradish peroxidase (HRP) (DakoCytomation, Glostrup, Denmark) or rabbit anti-mouse antibody conjugated-HRP (DakoCytomation, Glostrup, Denmark). Actin in each sample was detected as an internal control by using mouse anti-actin antibody (Sigma-Aldrich, Missouri, USA) and rabbit anti-mouse antibody conjugated-HRP (DakoCytomation, Glostrup, Denmark). Chemiluminescent signals generated by SuperSignal West Pico

Chemiluminescent Substrate (Thermo Scientific, Illinois, USA) were detected by using a G:BOXchemiluminescence imaging system (Syngene, Cambridge, UK).

**Plasmid constructs, cell culture and transfections**

The wild-type constructs, pcDNA5_$Na_V1.8$ and pcDNA5_$Na_V1.8$-venus, and reported gain-of-function mutation, pcDNA5_$Na_V1.8$_I1706V, were previously reported.[12,13] The wild-type constructs were used as templates to generate mutant constructs by PCR and site-directed mutagenesis method using *Pfx* DNA polymerase (Invitrogen, Carlsbad, CA, USA). Three additional mutant constructs, p.N909K, p.K1809R, and p.N909K/K1809R, of *SCN10A* were generated by the same method. This part of work was conducted at the Division of Molecular Medicine, Faculty of Medicine Siriraj Hospital, Mahidol University, Bangkok, Thailand. All mutant constructs were confirmed by Sanger DNA sequencing (First BASE Laboratories SdnBhd, Selangor, Malaysia).

HEK293 cells stably expressed SCN1B (HEK293-1B) generated for studying $Na_V1.8$ α subunit expression were cultured in Dulbecco's Modified Eagles Medium-F12 (DMEM-F12) supplemented with 10% (v/v) fetal bovine serum, 1.2% (v/v) pencillin-streptomycin solution (100 U/ml penicillin and 100 μg/ml streptomycin), and 200 μg/ml of G418 in a humidified $CO_2$ (5%) incubator at 37°C. The HEK293-1B cells were transfected with the wild-type or mutant plasmid constructs by using Lipofectamine™ 2000 (Invitrogen, Carlsbad, CA) according to manufacturer's instructions. The transfected cells were additionally incubated at 37°C, $CO_2$ for 48 hours prior to further investigations.

**Immunohistochemistry staining**

Human kidney tissues from remaining biopsy specimens were fixed in 4% paraformaldehyde and embedded in paraffin blocks. Then, 4-μm-thick tissues were serially cut from paraffin blocks and mounted onto glass slides coated with 1% (W/V) gelatin solution. After deparaffinization and rehydration, the kidney tissue sections were placed in sodium citrate buffer (10 mM sodium citrate, 2 mM EDTA, 0.05% tween-20,

pH 6.0) and subjected to heat retrieval at 70°C for 20 minutes. The sections were allowed to cool to room temperature and endogenous peroxidase activity was blocked by 3% hydrogen peroxide for 30 minutes. The sections were placed in 2% BSA for 30 minutes to block nonspecific bindings and incubated with a rabbit antibody against either $Na_V$ 1.8 α subunit (1:20) (Abcam, Cambridge, UK), AQP1 (1:200) or AQP2 (1:50) in PBS/2% (w/v) BSA overnight. Normal rabbit IgG (Cell Signaling Technology, USA) in equal concentration to the primary antibody was used as isotype control. After washing, secondary antibody (swine) against rabbit antibody conjugated with horseradish peroxidase (HRP, Dako, Japan) at dilution 1:200 in PBS/2% BSA was applied and incubated for 6 hours. The sections were washed and the color was developed by incubating in 0.03% 3.3-diaminobenzidine tetrahydrochloride (DAB) for at least 2 minutes and counterstained with hematoxylin and eosin (H&E). The tissue sections were then mounted with xylene-based mounting medium (Leica Biosystems, Illinois, USA) and viewed under a Nikon Eclipse TE200 inverted fluorescent microscope (Nikon, Tokyo, Japan).

**Double immunofluorescence staining**

The human fresh-frozen kidney tissues were sliced into 2-4 μm thickness by a rotary microtome. The tissue section was placed on a glass slide and fixed with acetone for 10 minutes before incubation with rabbit anti-human $Na_V1.8$ α subunit of voltage-gated sodium channel (Alomone, Jerusalem, Israel) and mouse anti-alpha 1 $Na^+/K^+$ATPase (Abcam, Cambridge, UK) as the primary antibodies, followed by incubation with donkey anti-rabbit IgG conjugated with Alexa 488 fluorescein and goat anti-mouse IgG conjugated with Cy3 fluorescein (Invitrogen, California, USA) as the secondary antibodies. The tissue sections were then incubated with PBS containing Hoechst 33258 (Molecular Probes), washed with PBS, and mounted with Fluorosave (DakoCytomation, Glostrup, Denmark). The stained tissue section was examined under a Olympus BX51 fluorescence microscope (Olympus, Tokyo, Japan).

**Quantitative western-blot analysis**

For quantitative Western-blot analysis, the transfected HEK293-1B cells were lysed with 100 µl of homogenization buffer [containing 150 mM NaCl, 1% Triton X-100, 20 mM Tris HCl (pH 7.5), 1 mM EDTA, 1 mM DTT, and 1x complete mini protease inhibitor (Sigma-Aldrich)], incubated and rotated at 4°C at least 30 minutes. Samples were centrifuged at 15,000 g for 20 minutes at 4°C, and the supernatant fraction was collected as total protein extraction. After quantification of the protein concentration by the Bradford assay (Bio-Rad), 0.5, 1.0 and 1.5 ug of proteins were separated by 4-12% SDS-PAGE, followed by electrophoretic transfer onto a nitrocellulose membrane and immunoblot analysis with the mouse anti-Pan Sodium Channel antibody and rabbit anti-actin antibody (Sigma-Aldrich, Missouri, USA) at 1:1,000 dilution.

**Electrophysiological study**

Transfected cells, which had been in 200 µg/ml G418 and 1 mM lidocaine for 24 hours (48 hours after transfection), were plated onto poly-L-lysine-coated cover slips ($1x10^5$ cells per 35-mm Petri dish; lidocaine was still present), and left overnight (10-12 hours). Then, they were exposed to culture media without lidocaine for at least three hours before subjected to an electrophysiological experiment. Whole-cell patch-clamp recording was conducted at room temperature (25-26°C), using an Axopatch 200B patch-clamp amplifier (Axon Instruments, Foster City, CA, USA) and a Digidata 1440A analog-to-digital converter (Axon Instruments). The pipette solution contained 120 mM CsF, 15 mM NaCl, 10 mM HEPES, and 10 mM EGTA (pH 7.25 with CsOH). The extracellular bath solution contained 140 mM NaCl, 4.7 mM KCl, 1 mM $CaCl_2$, 1.3 mM $MgCl_2$, 5 mM HEPES, and 11 mM glucose (pH 7.4 with NaOH). To block endogenous tetrodotoxin (TTX)-sensitive $Na^+$ currents, 0.3 µM TTX was always included in the bath solution to block tetrodotoxin-sensitive ($Na_V1.7$, $Na_V1.2$, $Na_V1.3$) and the tetrodotoxin-resistant $Na_V1.5$ which is expressed at low and variable levels in these cells[14] and would be 60% inactivated at -80 mV, according to Wang et al., 2015.[15] Pipette resistance was 3.50 ± 0.08 MΩ (mean ± SEM), yielding maximal voltage errors of -2.46 ±

0.10 mV. Pipette potential was adjusted to zero before seal formation; liquid junction potential was not corrected. Holding potential ($V_h$) was -80 mV.

Currents were measured after leak subtraction. Current–voltage (I–V) curves were constructed from peak currents in response to a series of 100-ms step depolarization, at 5 s intervals, from -80 mV $V_h$ to potentials between -60 and +60 mV, in 10 mV increments. Current density was calculated by normalizing peak currents with cell capacitance. Conductance (G) at each voltage (V) was calculated using the equation $G = I / (V\text{-}V_{rev})$ (I, peak current; $V_{rev}$, reversal potential). Individual conductance-voltage curve was plotted and fitted with a Boltzmann equation:

$$G = Gmin + \frac{Gmax - Gmin}{1 - exp\,\frac{V_{1/2} - V}{k}}$$

where conductance (G) is a function of the membrane potential (V); $V_{1/2}$ is the half maximal activation voltage; and k is the slope factor. Average $V_{1/2}$ and k of each group was used to construct the group's conductance-voltage curve.

Steady-state fast inactivation was assessed with a series of 500-ms prepulses (-90 to +10 mV in 5-mV increments) followed by a 40-ms test pulse to 0 mV to assess the available channels. Slow inactivation was assessed with 30-s prepulses at potentials ranging from -110 to +20 mV, followed by a 30-ms hyperpolarization at -80 mV to allow channel recovery from fast inactivation, and a 50-ms test pulse to 0 mV. Peak inward currents obtained during test pulses of steady-state fast-inactivation and slow-inactivation protocols were normalized to maximal peak current and fitted with the Boltzmann equation as a function of the inactivating voltage. Steady-state inactivation curves were constructed from average $V_{1/2}$ and k of each group.

The time constant of inactivation was obtained by fitting decaying currents with the standard exponential equation:

$$I = A * \exp(-t/\tau) + C$$

where A is the initial current amplitude, $t$ is time, $\tau$ is the time constant of decay, and C is the asymptotic minimum to which the currents decay. Persistent currents were measured as mean current amplitude between 93 and 98 ms after the onset of depolarization,[13] and are presented as percentage of the peak current.

Recovery of $Na_V1.8$ channels from fast inactivation was examined using a two-pulse protocol. A prepulse (100 ms, 0 mV) was followed by a test pulse (10 ms, 0 mV), with interpulse intervals varying from 2 to 600 ms (-80 mV). Recovery rates were measured by normalizing peak current during the test pulse to that during the prepulse. Recovery time constants were calculated using two-phase exponential association. All curve-fitting were done using GraphPad PRISM 5® (GraphPad Software, San Diego, CA, USA).

**Statistics**

Data sets were collected from at least three independent experiments. Values are expressed as mean ± SEM (standard error of the mean). Kolmogorov–Smirnov test was used to test the normality of all data sets. Either unpaired t-test or Mann–Whitney U test, as appropriate, was employed to compare the mean between two different groups. One-way analysis of variance (ANOVA) followed by the Sidak's multiple comparison test was used for statistically significant differences between the means of two or more independent groups. Differences with $p < 0.05$ were considered statistically significant.

**References**


1. Lindner, T.H. & Hoffmann, K. easyLINKAGE: a PERL script for easy and automated two-/multi-point linkage analyses. *Bioinformatics* **21**, 405-7 (2005).
2. Adzhubei, I.A. *et al.* A method and server for predicting damaging missense mutations. *Nat Methods* **7**, 248-9 (2010).
3. Cheng, Y.C. *et al.* VarioWatch: providing large-scale and comprehensive annotations on human genomic variants in the next generation sequencing era. *Nucleic Acids Res* **40**, W76-81 (2012).
4. Schwarz, J.M., Rodelsperger, C., Schuelke, M. & Seelow, D. MutationTaster evaluates disease-causing potential of sequence alterations. *Nat Methods* **7**, 575-6 (2010).
5. Kumar, P., Henikoff, S. & Ng, P.C. Predicting the effects of coding non-synonymous variants on protein function using the SIFT algorithm. *Nat Protoc* **4**, 1073-81 (2009).
6. Reva, B., Antipin, Y. & Sander, C. Predicting the functional impact of protein mutations: application to cancer genomics. *Nucleic Acids Res* **39**, e118 (2011).
7. Chun, S. & Fay, J.C. Identification of deleterious mutations within three human genomes. *Genome Res* **19**, 1553-61 (2009).
8. Cartegni, L., Wang, J., Zhu, Z., Zhang, M.Q. & Krainer, A.R. ESEfinder: A web resource to identify exonic splicing enhancers. *Nucleic Acids Res* **31**, 3568-71 (2003).
9. Nettuwakul, C., Sawasdee, N. & Yenchitsomanus, P.T. Rapid detection of solute carrier family 4, member 1 (SLC4A1) mutations and polymorphisms by high-resolution melting analysis. *Clin Biochem* **43**, 497-504 (2010).
10. Reed, G.H., Kent, J.O. & Wittwer, C.T. High-resolution DNA melting analysis for simple and efficient molecular diagnostics. *Pharmacogenomics* **8**, 597-608 (2007).
11. Neff, M.M., Neff, J.D., Chory, J. & Pepper, A.E. dCAPS, a simple technique for the genetic analysis of single nucleotide polymorphisms: experimental applications in Arabidopsis thaliana genetics. *Plant J* **14**, 387-92 (1998).

12. Faber, C.G. *et al.* Gain-of-function Nav1.8 mutations in painful neuropathy. *Proc Natl Acad Sci U S A* **109**, 19444-9 (2012).

13. Huang, J. *et al.* Small-fiber neuropathy Nav1.8 mutation shifts activation to hyperpolarized potentials and increases excitability of dorsal root ganglion neurons. *J Neurosci* **33**, 14087-97 (2013).

14. He, B. & Soderlund, D.M. Human embryonic kidney (HEK293) cells express endogenous voltage-gated sodium currents and Na v 1.7 sodium channels. *Neurosci Lett* **469**, 268-72 (2010).

15. Wang, Y., Mi, J., Lu, K., Lu, Y. & Wang, K. Comparison of Gating Properties and Use-Dependent Block of Nav1.5 and Nav1.7 Channels by Anti-Arrhythmics Mexiletine and Lidocaine. *PLoS One* **10**, e0128653 (2015).